Journal of Catalysis **199,** 60–72 (2001)
doi:10.1006/jcat.2000.3143, available online at http://www.idealibrary.com on IDEAL®

Study of the Co–Pt Synergism for the Selective Catalytic Reduction of NO_x with CH_4

L. B. Gutierrez,* A. V. Boix,* E. A. Lombardo,*,[1] and J. L. G. Fierro†

*Instituto de Investigaciones en Catálisis y Petroquímica-INCAPE-(FIQ, UNL-CONICET), Santiago del Estero 2829, 3000 Santa Fe, Argentina; and †Instituto de Catálisis y Petroleoquímica, Cantoblanco, 28049 Madrid, Spain

Received August 14, 2000; revised November 27, 2000; accepted December 7, 2000

The selective catalytic reduction of NO_x with CH_4 in excess oxygen with or without added water was conducted over a series of ion-exchanged mordenites. The fresh catalysts contained both Pt and Co cations in varying proportions. Different treatments of the solid either after or between exchanges were performed in order to learn about the beneficial effect of Pt added to Co-mordenite. Temperature-programmed reduction of the solids together with photoelectron spectroscopy provided information concerning the interaction, migration, and oxidation states of Co and Pt. These studies were performed over the fresh, reduced, and used catalysts. The best formulations have Co/Pt atomic ratios between 15 and 24 and they exhibit better water resistance than Co-mordenites.

Key Words: **NO_x reduction, PtCo-mordenite; SCR; Pt–Co synergism.**

INTRODUCTION

The use of Co-zeolites in the selective catalytic reduction of NO_x with methane is limited by the detrimental effect of both H_2O and SO_2 (1, 2) on these catalysts. On the other hand, Pt-containing catalysts are highly resistant to both of them (3, 4) but such catalysts are not selective when methane is the reductant. Furthermore, they are active in the oxidation of SO_2 to SO_3 and show high selectivity to N_2O. If the good properties of Co- and Pt-based catalysts could be enhanced and the negative features kept to a minimum, one would have at hand a superior catalytic system. With this in mind, Petunchi and co-workers studied Pt, Co-zeolite catalysts applied to the selective catalytic reduction (SCR) of NO_x with methane (5, 6).

In a recent paper, Gutierrez *et al.* (7) investigated whether the good results obtained with PtCo-zeolites could be achieved or even improved by using either alumina, a mechanical mixture of Pt- and Co-zeolites, or two-bed reactors. None of these options worked better than the PtCo-mordenite in which both cations were exchanged and probably homogeneously distributed inside the zeolite structure. The best catalyst was obtained with Co/Pt = 15 (atomic ratio) prepared by ion exchange and reduced in flowing hydrogen at 623 K before use. The authors concluded that the type of interaction was unknown and more research was needed to explain this phenomenon. Thus, this work was undertaken trying to understand the nature of the Co–Pt interaction through the use of additional characterization tools, particularly X-ray photoelectron spectroscopy.

[1] To whom correspondence should be addressed. Fax: 54-342-4536861. E-mail: nfisico@fiqus.unl.edu.ar.

EXPERIMENTAL

Catalysts Preparation and Pretreatment

Catalysts were prepared by ionic exchange starting from Na-mordenite (Na-mor) of unit cell composition, $Na_7(AlO_2)_7(SiO_2)_{41}$. The catalysts prepared are shown in Table 1. Monometallic Pt-mor and Co-mor solids were prepared using $Pt(NH_3)_4(NO_3)_2$ and $Co(NO_3)_2$, respectively. The exchange time was 24 h at room temperature and then the solids were filtered, washed, and dried at 393 K for 8 h. Pt-mor was calcined in O_2 at a heating rate of 0.5 K/min up to 623 K, keeping this temperature for 2 h. Co-mor was conditioned following the standard pretreatment, i.e., heating at 2 K/min in O_2 flow up to 673 K with three isothermal legs, at 383 K and 483 K for 2 h each, and at 673 K for 8 h. For the PtCo-mor systems, the Na-mor was exchanged with $Pt(NH_3)_4(NO_3)_2$, dried, and subjected to a second exchange with $Co(NO_3)_2$. Prior to the catalytic tests these solids were pretreated as the Pt-mor. Other binary Pt^*Co-mor and Co^*Pt-mor samples were also prepared. For Pt^*Co-mor, Pt-exchanged samples were calcined in O_2 at a slow heating rate (0.5 K/min) and then reduced with flowing H_2 for 1 h at 623 K. Following this treatment the Co^{2+} was exchanged and conditioned by following the standard pretreatment. Finally, for the Co^*Pt-mor sample, Co^{2+} was exchanged in mordenites as before, calcined in O_2 (standard pretreatment), and then the exchange with Pt was performed. After that, the solids were again calcined in O_2 at 623 K (at 0.5 K/min).

0021-9517/01 $35.00

TABLE 1

Catalyst Composition

Catalyst[a]	Metal,[b] μmol Co	Pt
$Pt_{0.37}$-mor	—	1.9
$Pt_{0.73}$-mor	—	3.7
$Pt_{1.85}$-mor	—	9.5
$Co_{1.19}$-mor	20.2	—
$Co_{2.91}$-mor	49.3	—
$Pt_{0.31}Co_{1.40}$-mor(15)	23.7	1.6
$Pt_{0.73}Co_{2.60}$-mor(11.7)	44	3.7
$Pt_{1.14}Co_{2.92}$-mor(8.5)	49.5	5.8
$Pt_{4.7}Co_{0.8}$-mor(0.56)	24.1	13.6
$Pt_{0.21}Co_{3.04}$-mor(48)	51.5	1.08
$Pt_{0.39}Co_{2.87}$-mor(24)	48.6	2.0
$Co_{2.6}Pt_{0.41}$-mor(20)	44.1	2.1
$Pt_{0.30}Co_{1.83}$-Hmor(20)	30.8	1.54
$Pt^{*}_{0.43}Co_{1.31}$-mor(10)	22.2	2.2
$Co^{*}_{2.06}Pt_{0.69}$-mor(10)	35	3.5

[a] Subindexes indicate the wt% of metal. The Co/Pt ratio is given in parentheses.

[b] Amount of metal per 100 mg of catalyst.

Catalytic Measurements

The reaction was carried out using 0.5 g of catalyst placed on a fixed-bed flow reactor. This was a 12-mm-i.d. tubular quartz reactor. The typical reacting mixture consisted of 1000 ppm of CH_4, 1000 ppm of NO, and 2% O_2 balanced at 1 atm with He (GHSV, 6500 h^{-1} referred to the same total weight of the catalyst). Water was introduced through a saturator. The catalytic activity was evaluated with an SRI 9300B chromatograph with two columns, 5 Å molecular sieve, and Chromosorb 102. The NO_x conversion (C_{NO}) was calculated from N_2 production: $C_{NO} = 2[N_2]/[NO]^{\circ} \times 100$, where $[NO]^{\circ}$ is the NO initial concentration. The CH_4 conversion (C_{CH_4}) was obtained as $C_{CH_4} = ([CH_4]^{\circ} - [CH_4])/[CH_4]^{\circ} \times 100$. Selectivity ($s$) was defined as $s(\%) = 0.5C_{NO}/C_{CH_4} \times 100$.

The turnover frequencies were calculated as follows. The rate was obtained by increasing the GHSV up to 100,000 h^{-1} in order to keep the NO conversion below 20%. The number of active sites was assumed to be equal to the concentration of Co^{2+} exchanged in the zeolite lattice following the criteria used by Li and Armor (8).

TPR Experiments

These experiments were performed with 100 mg of catalyst using an Okhura TP-2002 S instrument equipped with a TCD detector. The reducing gas was 5% H_2 in Ar, flowing at 30 mL/min, and the heating rate was 10 K/min.

Surface Analysis by XPS

X-ray photoelectron spectra were acquired with an ESCALAB 200R electron spectrometer equipped with a hemispherical electron analyzer and an Al$K\alpha$ X-ray source ($h\nu = 1486.6$ eV). The Si 2*p*, Al 2*p*–Pt 4*f*, Pt 4*d*, Co 2*p*, O 1*s*, and C 1*s* core-level spectra were recorded for all the samples. As the Co 2*p* and Pt 4*d* signals were very weak, the corresponding energy regions were scanned 200 times in order to improve the signal-to-noise ratio. All the peaks were fitted by a Gaussian–Lorentzian component waveform after an inelastic (Shirley-type) background had been subtracted. For the Al 2*p* and Pt 4*f* peaks the situation was more complex because they overlapped. In order to analyze the contribution of the two elements, it was assumed that (i) the BE and FWHM of the Al 2*p* peak were the same as in the unloaded zeolite and (ii) the spin–orbit splitting for Pt was fixed to 3.35 eV and the Pt $4f_{5/2}$/Pt $4f_{7/2}$ intensity ratio was kept constant (0.75). In order to calculate the surface atomic ratio (n_i/n_j) the following equation was used,

$$n_i/n_j = (I_i/I_j)(\sigma_j/\sigma_i)(\mathrm{KE}_i/\mathrm{KE}_j)^{1/2},$$

where I is the intensity of the peak, σ is the lonization cross section, and KE is the kinetic energy of the element i or j, respectively. The samples calcined and the catalysts used in the SCR reaction were dehydrated in a vacuum (10^{-5} Torr), followed by heating at a rate of 5 K/min up to 623 K to remove adsorbed water. The calcined samples were reduced in H_2 for 1 h at 623 K. The dehydration and reduction treatments were conducted within the pretreatment chamber of the spectrometer so that the solid would not be in contact with the atmosphere. The binding energy values of the Al 2*p* (74.5 eV), O 1*s* (532.5 eV) electronic levels stayed constant for mono- and bimetallic solids within the experimental error (±0.1 eV) and the BE of Si 2*p*, 103.0 eV, was adopted as an internal reference.

RESULTS

Catalytic Behavior

1. Monometallic catalysts. Co-mordenite. The standard activity test was run using a gas stream containing 2% O_2 and 1000 ppm each of NO and CH_4. With a GHSV of 6500 h^{-1} the calcined $Co_{1.19}$-mor yielded a maximum NO to N_2 conversion of 30% at 723 K while the conversion of CH_4 to CO_2 reached 45% at the same temperature. When the catalyst was pre-reduced at 623 K in pure flowing H_2 for 1 h, the selectivity significantly dropped, reaching a conversion of NO to N_2 of 18% at 723 K using the same feed stream. The $Co_{2.91}$-mor exhibited a similar catalytic behavior.

Pt-mordenite. When $Pt_{0.37}$-mor was assayed under the same conditions as above, it showed no N_2 formation between 373 and 773 K. At the higher end, it became active for methane combustion. At 773 K, methane conversion was 60%. The reduction treatment did not improve the performance of this catalyst.

2. Bimetallic catalysts. The mordenites containing both Pt and Co showed different catalytic behavior depending

on the Co/Pt atomic ratio and the presence or absence of water. The effect of treatments between the exchange of both cations was also investigated. The results obtained are described below.

Effect of the Co/Pt ratio. In previous studies Gutierrez *et al*. (5–7) have shown that the reduction of the catalyst in H_2 at 623 K greatly enhances the selectivity toward N_2 production of these catalysts. Thus, all the formulations assayed were prereduced in H_2 at 623 K. On the other hand, when the catalyst was reduced at 973 K, the maximum NO conversion was only 10% at 773 K while CH_4 was totally burned at the same temperature. Figure 1 shows the maximum conversion of NO to N_2 observed between 723 and 773 K on nine bimetallic catalysts. The catalyst containing 0.31% of Pt was the most selective, reaching 80% conversion to N_2 at 773 K. In all cases but one, it was observed that the addition of Pt enhanced the activity of the Co-mor. The exception was the formulation containing 4.7% Pt.

Observing the performance of the catalysts with similar cobalt loading (2.5–2.9%), it is concluded that the best selectivity is achieved when the Pt/Co ratio is within 0.03 to 0.06 (Fig. 1A). Similarly, when the Pt loading is kept roughly constant (Fig. 1B) the best catalysts have a Co/Pt ratio between 15 and 24. Table 2 also confirms that the PtCo-mor (15) gives the highest TOF for NO_x reduction at 623–673 K.

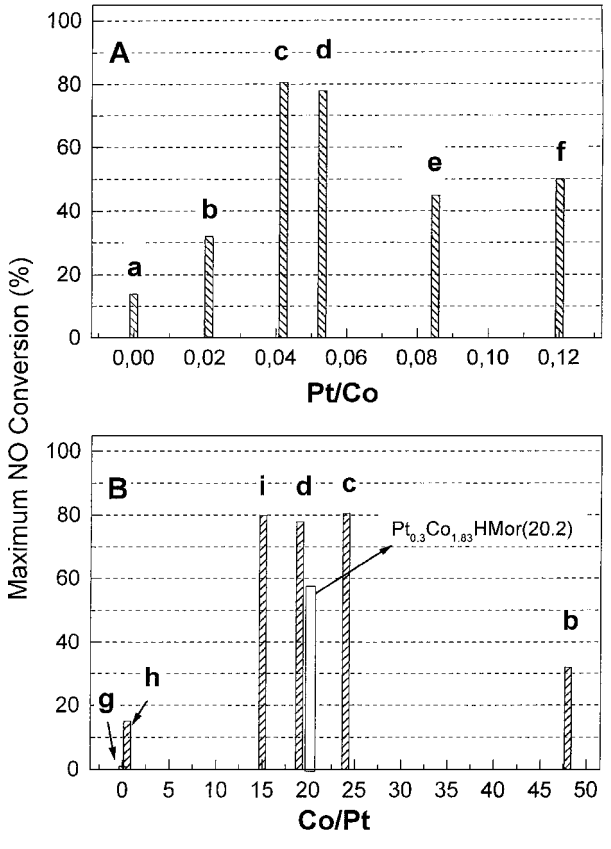

FIG. 1. Effect of the metallic ions loading on the maximum NO to N_2 conversion (observed at 723–773 K): (A) nearly constant Co loading; (B) nearly constant Pt loading. (a) $Co_{2.91}$-mor, (b) $Pt_{0.21}Co_{3.04}$-mor(48), (c) $Pt_{0.39}Co_{2.87}$-mor(24), (d) $Co_{2.60}Pt_{0.41}$-mor(20), (e) $Pt_{0.73}Co_{2.60}$-mor(11.7), (f) $Pt_{1.14}Co_{2.92}$-mor(8.5), (g) $Pt_{0.37}$-mor, (h) $Pt_{4.7}Co_{0.8}$-mor(0.56), and (i) $Pt_{0.31}Co_{1.40}$-mor(15). Reaction conditions: $[O_2]$, 2%; $[NO]=[CH_4]=$ 1000 ppm; GHSV, 6500 h^{-1}.

TABLE 2

Turnover Frequencies of Pt_xCo_y-mor for NO_x Reduction[a]

	TOF × 10^4, (s^{-1})			
	Dry		Wet (2% H_2O)	
Catalyst	623 K	673 K	623 K	673 K
$Pt_{0.31}Co_{1.40}$-mor(15)	1.43	3.4	0	1.43
$Pt_{0.73}Co_{2.6}$-mor(11.7)	0.5	1.3	0	0.70
$Pt_{4.14}Co_{2.92}$-mor(8.5)	0.8	1.8	0	0.27
$Co^*_{2.06}Pt_{0.69}$-mor(10)	0.30	1.2	0.17	0.46
$Pt^*_{0.43}Co_{1.31}$-mor(10)	0.33	1.6	0	0.27
$Co_{2.91}$-mor	0	1.1	0	0
$Co_{1.19}$-mor	0	1.6	0	0

[a] Reaction conditions: $[NO]=[CH_4]=1000$ ppm, $[O_2]=2\%$, GHSV between 6500 h^{-1} and 100,000 h^{-1} to keep NO conversion below 20%.

It is generally accepted that during H_2 reduction, Brønsted acid sites are formed (9). Thus, a catalyst was prepared starting from NH_4-mor with a Co/Pt ratio of 20 (Fig. 1B). The lower conversion to N_2 seemed to indicate that the presence of protons does not play a significant role in the Co,Pt system.

Effect of water. Four of the formulations shown in Fig. 1 were selected to investigate the effect of water on the catalytic behavior. Figures 2 and 3 show the effect of water on NO conversion. At high reaction temperatures, the NO conversion was higher for catalysts with high Co/Pt ratios (15, 11.7) while at lower temperatures this trend was not observed (Fig. 2). The same overall trend was observed with methane conversion (not shown). When the water addition was stopped the catalysts recovered their activities. Figure 3 shows that the presence of protons in the catalyst does not affect the water resistance of the bimetallic catalysts. The recovery of the catalyst activity upon returning to the dry feed stream is shown in Fig. 3.

Table 2 gives a quantitative measure of the effect of water upon the reaction rates for NO reduction. The monometallic catalysts are much more sensitive to the presence of water than the bimetallic ones. This is also supported by the data in Fig. 2 which evidence the increased sensitivity to water of the $Co_{1.19}$-mor compared to $Pt_{0.31}Co_{1.40}$-mor(15). Additionally, the difference between dry and wet data almost disappears at 823 K for the bimetallic catalysts, but is still significant for the Co-mor.

Treatments between exchanges. A set of bimetallic catalysts was prepared by successive exchanges, but before

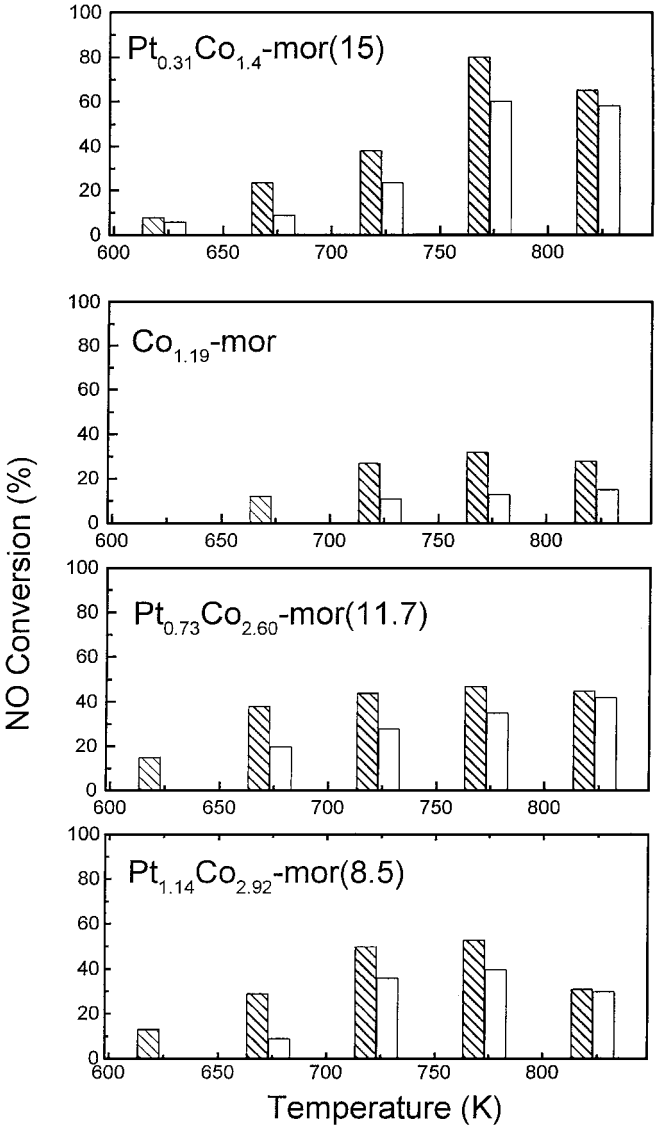

FIG. 2. Effect of steam on NO conversion over PtCo-mor and Co-mor catalyst. Striped bars, 0% H_2O; empty bars, 2% H_2O. Reaction conditions as in Fig. 1.

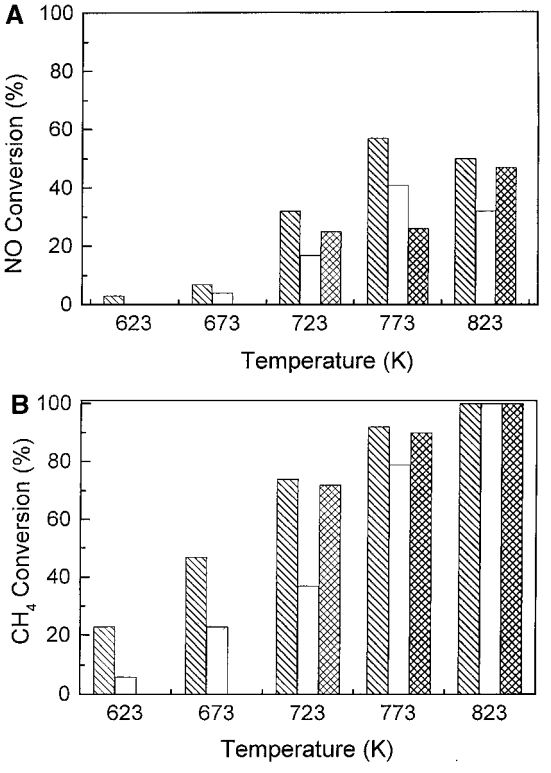

FIG. 3. Catalytic activity of $Pt_{0.30}Co_{1.83}$-Hmor (20.2) catalyst: (A) NO to N_2 conversion; (B) CH_4 to CO_2. Striped bars, 0% H_2O; empty bars, 2% H_2O; cross-striped bars, 0% H_2O, after removing water from reaction stream. Reaction conditions as in Fig. 1.

The intermediate calcination and/or reduction modifies the characteristics of the species present in the zeolitic structure in such a way that the Pt and Co species tend to segregate from each other. Let us see if the TPR and XPS observations substantiate this hypothesis.

the second exchange the monometallic solid was either calcined and/or reduced (see Experimental). Figure 4A shows the catalytic behavior of reduced Co^*Pt-mor(10) and Pt^*Co-mor(10) under both dry and wet conditions. Note that the latter is much more affected by the presence of water than the former. Consistent with this observation is the effect of water upon the rate of reaction shown in Table 2. However, Pt^*Co-mor is still more resistant to water than the monometallic Co-mordenites (Table 2 and Fig. 2). Figure 4B shows that the calcined Pt^*Co-mor(10) behaves similarly to the reduced Co^*Pt-mor(10). This means that the Pt^*Co-mor is adversely affected by reduction, a behavior similar to that of Co-mordenites and opposite to that of PtCo-mordenites.

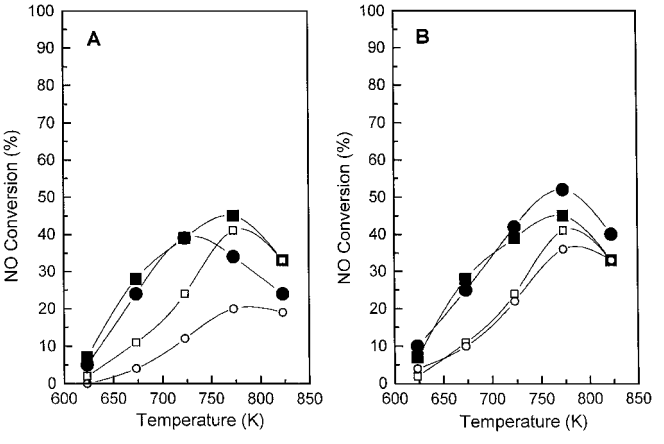

FIG. 4. Effect of treatments between exchanges on the catalytic behavior: (A) ■, □, Co^*Pt-mor (reduced), and ●, ○, Pt^*Co-mor (reduced). (B) ●, ○, Pt^*Co-mor (calcined), and ■, □, Co^*Pt-mor (reduced). Reaction conditions as in Fig. 1. Empty symbols, 0% H_2O; full symbols, 2% H_2O.

TPR Data

TPR experiments provide information on the effect of the reacting atmosphere on the reducibility of the bimetallic catalysts. In-depth analysis of the TPR data might well be used to extract information on the interaction between the mordenite lattice with Co and Pt, the presence of segregated metal oxides, and the type of interaction between Pt and Co. Two sets of TPR data were obtained: (i) reducibility of fresh and used bimetallic catalysts and (ii) effect of different treatments upon reducibility.

Reducibility of fresh and used bimetallic catalysts. Figure 5 shows the TPR profiles of four selected catalysts and Table 3 summarizes the reducibility of each one. All the fresh samples show similar profiles while the total H_2 consumption increases with Pt content for the fresh samples. From the data in Table 3 it is clear that H_2 consumption of the bimetallic catalysts is larger than the sum of the H_2 consumption of the Pt- and Co-monometallic ones. The maximum of the peaks is also different. These results indicate that Co reducibility increases sharply when Pt is present. As a matter of fact, the total H_2 consumption per mole of Co is larger than unity for catalysts with Co/Pt = 15, 8.5, and 0.56, which means that the average oxidation state of either Co or Pt, or of both, must be higher than 2. The exception is the sample Co/Pt = 11.7 in which the $H_2/(Co + Pt)$ ratio is 0.85. Particularly, in Co/Pt = 0.56 the high consumption at low temperature (Table 3) suggests the presence of

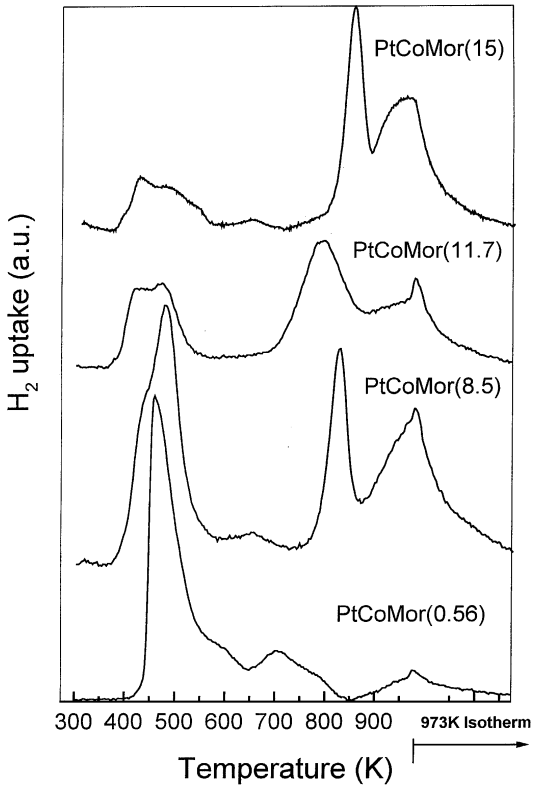

FIG. 5. Effect of the Pt/Co ratio on the reducibility of fresh PtCo-mor. TPR conditions: 30 mL/min of H_2 (5%)/Ar, 10 K/min up to 973 K.

TABLE 3

Reducibility of Fresh Mono- and Bimetallic Catalysts

Catalyst	Pt,[a] μmol	Co,[a] μmol	$H_2/(Co + Pt)$[b]	H_2/Co[c] (K)[d] Peak 1	Peak 2	Peak 3	Peak 4
$Co_{2.91}$-mor	—	49.3	0.34	—	0.05 (623)	—	0.29 (973)
$Co_{1.19}$-mor	—	20.2	0.62	—	—	—	0.62 (973)
$Pt_{0.37}$-mor	1.9	—	0.89	0.5[e] (523)	—	—	0.39[e] (943)
$Pt_{1.85}$-mor	9.5	—	1.28	0.97[e] (403)	—	0.31[e] (803)	—
$Pt_{0.31}Co_{1.40}$-mor(15)	1.6	23.7	1.11	0.07 (468)	0.02 (653)	0.41 (853)	0.62 (973)
$Pt_{0.73}Co_{2.60}$-mor(11.7)	3.7	44	0.85	0.16 (433)	—	0.39 (798)	0.28 (973)
$Pt_{1.14}Co_{2.92}$-mor(8.5)	5.8	49.5	1.15	0.36 (483)	0.08 (658)	0.24 (828)	0.48 (973)
$Pt_{4.7}Co_{0.8}$-mor(0.56)	24.1	13.6	1.84	1.86 (458)	0.92 (706)	—	0.55 (973)

[a] In 100 mg of catalyst.
[b] Total H_2 consumption per mole of Co + Pt.
[c] Pt reduction is subtracted from the total H_2 consumption.
[d] Temperature at the peak.
[e] H_2/Pt.

either Pt^{4+} or the formation of $PtCo_xO_y$ species (10). The H_2 consumption measured at temperatures around 673 K is indicative of the presence of cobalt oxides (Table 3). The two overlapping peaks at the high-temperature end, responsible for the reduction process $Co^{2+} + H_2 \rightarrow Co^{\circ} + 2H^+$, may be due to the location of Co^{2+} ions in two different sites (11–13).

The TPR data for the used catalysts (Fig. 6 and Table 4) show significant changes from those obtained with the fresh samples (Fig. 5). On the other hand, there are no major differences between the traces observed after reaction in either dry or wet streams. In all cases, a broad peak appears at the high-temperature end (Fig. 6). The peaks appearing at $T < 623$ K indicate that the species in the catalyst prereduced at 623 K has been reoxidized during reaction. The low-temperature peaks in the two samples with the highest Pt loading are again consistent with the presence of easily reducible species (probably oxides) which have migrated to the external surface of the zeolite crystals. On the other hand, the decrease in H_2 consumption between 673 and 873 K must be due to the migration of the exchanged species to less accessible sites (Fig. 6 and Table 4).

Effect of different treatments upon reducibility. TPR profiles were also recorded for the representative sample with Co/Pt = 15 reduced previously at 623 K and then reoxidized in O_2 at 823 K for 1 h (TPR_1 in Fig. 7). The H_2 consumption in Table 5 for the single, broad peak centered about 953 K is also observed for the same catalyst after reaction (Fig. 6 and Table 4).

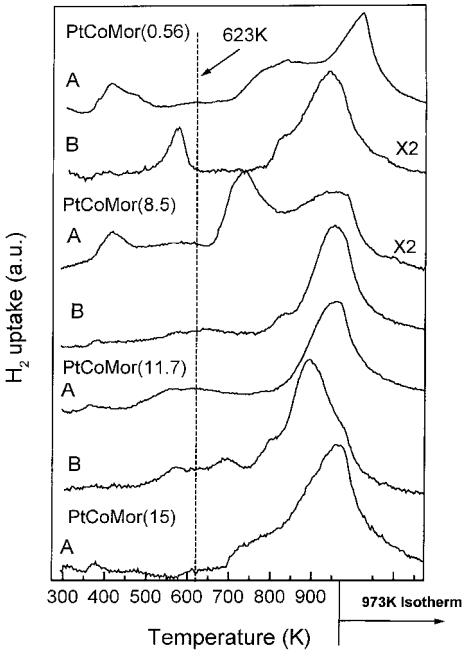

FIG. 6. Effect of the reacting gases on the PtCo-mor reducibility: (A) used under dry reaction conditions; (B) used under wet reaction conditions. The fresh catalysts have been reduced at 623 K before contacting the feed stream.

As the bimetallic samples reduced in H_2 at 973 K were found not to be active in the reaction, a fresh representative sample with Co/Pt = 15 was reduced in H_2 at 973 K and reoxidized in O_2 at 823 K. Its TPR profile (TPR_2 in Fig. 7)

TABLE 4

H_2 Consumption of Used PtCo-mor Catalysts

Used catalyst[a]		$H_2/(Co+Pt)$[b]	H_2, μmol (K)[c] Peak 1	Peak 2	Peak 3	Peak 4
$Pt_{0.31}Co_{1.40}$-mor(15)						
Pt: 1.6 μmol	Dry	1.11	—	—	—	26.5 (973)
Co: 23.7 μmol	2% H_2O	1.13	—	3.8 (623)	—	23.2 (893)
$Pt_{0.73}Co_{2.60}$-mor(11.7)						
Pt: 3.7 μmol	Dry	0.42	—	3.73 (573)	—	16.3 (960)
Co: 44 μmol	2% H_2O	0.45	—	3.9 (643)	—	17.6 (955)
$Pt_{1.14}Co_{2.92}$-mor(8.5)						
Pt: 5.8 μmol	Dry	0.94	5.9 (413)	—	22.3 (738)	23.8 (973)
Co: 49.5 μmol	2% H_2O	0.90	—	2 (573)	—	42 (943)
$Pt_{4.7}Co_{0.8}$-mor(0.56)						
Pt: 24.1 μmol	Dry	0.87	—	—	16 (843)	14 (1013)
Co: 13.6 μmol						

[a] Reaction conditions: O_2, 2%; [NO] = [CH_4] = 1000 ppm; GHSV, 6500 h^{-1}; H_2O, 2%.
[b] Total H_2 consumption per mole of (Co + Pt).
[c] Temperature at the peak.

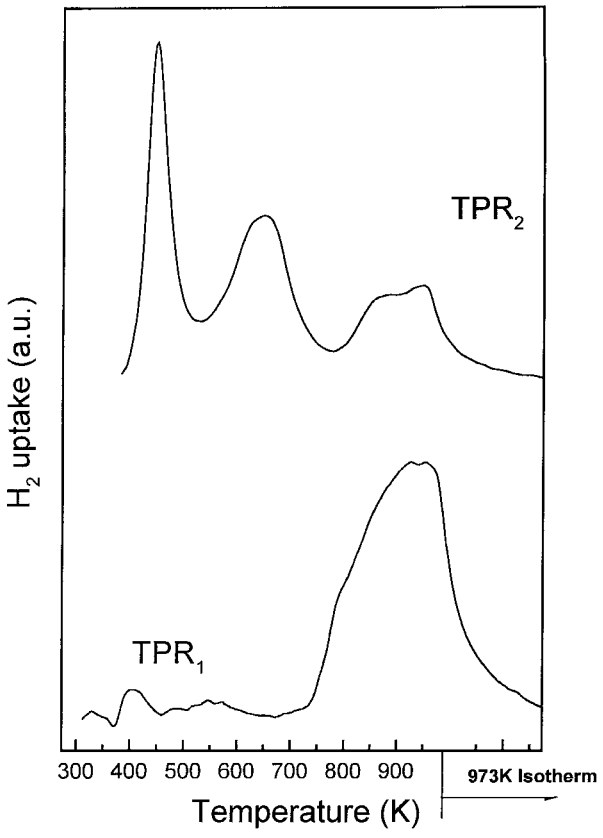

FIG. 7. Effect of the different treatments on $Pt_{0.31}Co_{1.40}$-mor(15) reducibility. TPR_1, reduced at 623 K; TPR_2, reduced at 973 K. In both cases the catalyst was reoxidized in O_2 at 823 K before running TPR experiments.

shows three reduction peaks. The first one at 448 K represents a consumption of 6.9 μmol for 100 mg of catalyst (Table 5). This amount is larger than expected for the total reduction of Pt^{2+} (2.5 μmol). Maybe these severe treatments lead to the formation of Pt^{4+}, $PtCoO_x$, cobalt oxides, or a combination thereof. The second peak at 648 K falls in the region corresponding to CoO and/or Co_3O_4. The third one belonging to Co^{2+} in exchange lattice sites is much smaller than that in the same solid after reduction at 623 K (see TPR_1 in Fig. 7). Thus, it is inferred that the inhibition of activity of the bimetallic catalysts reduced at 923 K is associated with a redistribution of Co^{2+} ions.

TABLE 5

Reducibility of $Pt_{0.31}Co_{1.40}$-mor(15) after Different Treatments

Fresh catalyst		$H_2/(Co+Pt)^a$	H_2/Co^a (K)^a Peak 1	Peak 2	Peak 3	Peak 4
$Pt_{0.31}Co_{1.40}$-mor(15)	$TPR_1{}^b$	0.88	—	—	—	0.89 (953)
	$TPR_2{}^c$	0.97	0.26 (448)	0.32 (648)	—	0.29 (898)

[a] See footnotes in Table 3.
[b] Catalyst was reduced at 623 K and reoxidized in O_2 at 823 K.
[c] Catalyst was reduced at 973 K and reoxidized in O_2 at 823 K.

Figure 8 shows the TPR profiles of Pt^*Co-mor(10) and Co^*Pt-mor(10). The profiles obtained with the used catalysts both in the presence and in the absence of water are almost identical. For the sake of simplicity, only the profiles corresponding to used catalysts under dry conditions are shown. By comparing fresh catalysts with similar Co/Pt ratios, some differences in the TPR profiles (Figs. 5 and 8) were found. The total H_2 consumption of both Co^* and Pt^* (fresh) was lower than those recorded in the PtCo-mor with similar Co/Pt ratios (Table 3 and 6). In the case of Co^*, the first peak is very similar to the one observed in $Pt_{1.85}$-mor (Table 3), suggesting the presence of Pt^{2+} in the bimetallic sample.

There is not much difference in the total hydrogen consumption of fresh Co^* and Pt^* (Table 6). A large difference is observed, however, in the low-temperature peak. This may suggest that the intermediate calcination and pre-reduction with H_2 of the Pt-mor impairs a close Pt–Co interaction, thereby limiting the ability of platinum to catalyze the reduction of Co^{2+} located at exchange positions.

All the used catalysts are harder to reduce than the fresh ones. Significant alterations of the TPR profiles are evident (Fig. 8). The reduced used Pt^* catalyst is now more difficult to reduce than the used Co^* (Table 6). The TPRs of the Pt^*Co-mor used catalysts show significant redistribution of reducible species. The low $H_2/(Co + Pt)$ ratio of 0.25 points to migration of species toward less reducible positions, and to migration of other species toward more easily reducible zones (the 773 K peak disappears and one appears at 623 K). The presence of Pt in both the Pt^* and Co^* samples increases the reducibility of Co but to a lesser extent than in the mordenites without intermediate treatment (Tables 3 and 6).

XPS Data

The surface features of both mono- and bimetallic mordenites were revealed by photoelectron spectroscopy.

$Co_{2.91}$-mordenite. The binding energies (BE) of Co $2p_{3/2}$ core-level spectra of this fresh sample after different treatments are summarized in Table 7. The main peak at ca. 782.4 eV is characteristic of Co^{2+}-exchanged zeolites (13–15). The peak at ca. 780.0 eV belongs to cobalt oxide. As the BEs for several cobalt compounds are very close, CoO (780.1 eV), Co_3O_4 (780.0 eV), and Co_2O_3 (780.0 eV) (16), our BE values cannot be assigned to a particular oxide. None of the treatments shown in Table 7 modify the XPS signal, which is consistent with the TPR data reported in Table 3. No, or very little, bulk reduction was detected at 623 K in the case of Co-mor. The surface atomic ratios calculated from the XPS data (Table 7) show that the cobalt

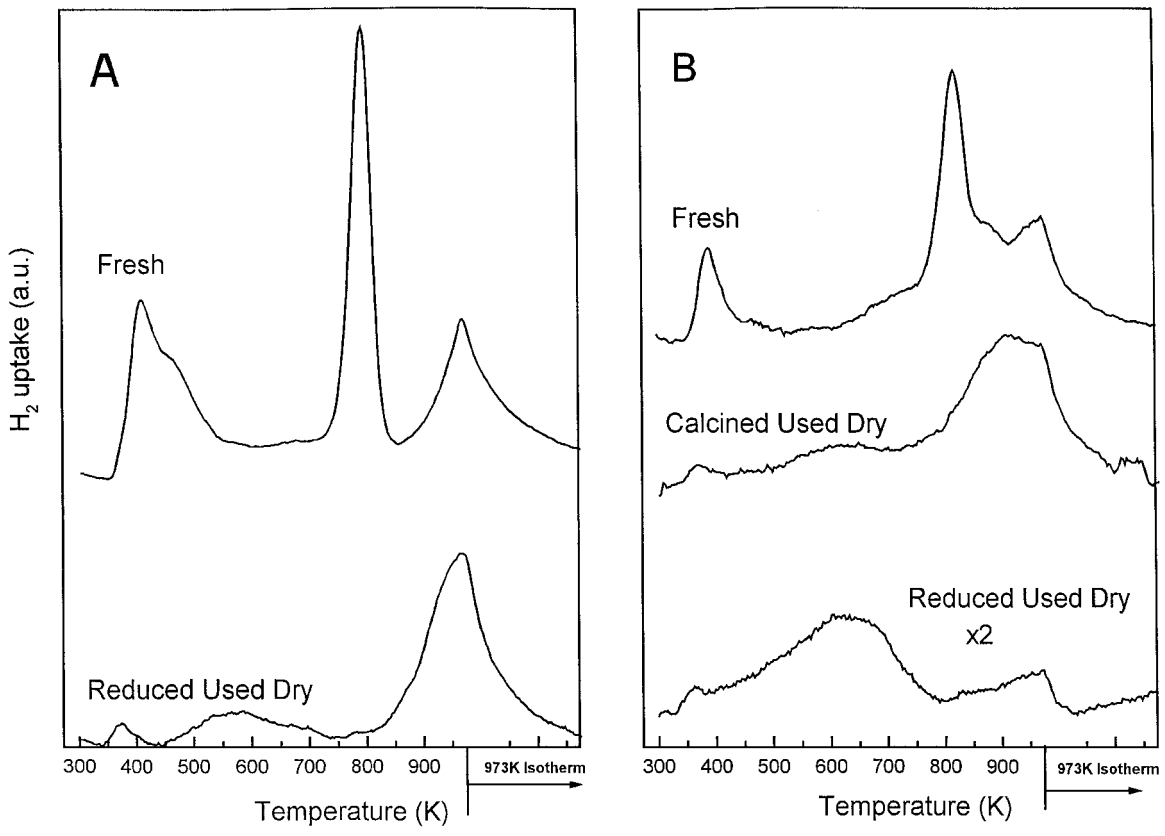

FIG. 8. TPR profiles of (A) $Co^{*}_{2.06}Pt_{0.69}$-mor(10) and (B) $Pt^{*}_{0.43}Co_{1.31}$-mor(10) samples (fresh and used).

in the fresh samples is concentrated on the surface. After the samples are exposed to reaction conditions, the cobalt migrates into the zeolite structure and the Co/Si ratio approaches that expected for an uniform distribution of Co within the lattice.

Pt-mordenite. For Pt-containing mordenites both Pt 4*f*, which overlaps with Al 2*p*, and Pt 4*d* peaks were recorded. Table 8 shows the XPS data for two Pt-mordenites. For the calcined $Pt_{0.37}$-mor sample the Pt $4f_{7/2}$ BE resulted in 72.4 eV, and shifted to 71.9 eV upon reduction. However,

TABLE 6

Reducibility of Bimetallic Catalysts with Intermediate Treatments

Catalyst	Treatment	$H_2/(Co+Pt)^a$	H_2 consumption[b] (K)[c]			
			Peak 1	Peak 2	Peak 3	Peak 4
$Co^{*}_{2.06}Pt_{0.69}$-mor(10)						
Pt = 3.5 μmol	Fresh	0.62	8 (410)	—	9 (798)	7 (973)
Co = 34.9 μmol	Reduced, used,[d] dry	0.35	0.5 (373)	2.7 (573)	—	10.6 (973)
$Pt^{*}_{0.43}Co_{1.31}$-mor(10)						
Pt = 2.2 μmol	Fresh	0.77	2.1 (388)	—	11 (823)	5.9 (973)
Co = 22.2 μmol	Calcined. used,[d] dry	0.49	—	1.9 (623)	—	10.4 (923)
	Reduced, used,[d] dry	0.25	—	4.6 (623)	—	1.2 (973)

[a] Total H_2 consumption per mole of (Co + Pt).
[b] Micromoles of H_2.
[c] Temperature at the peak.
[d] Reaction conditions: see Fig. 1.

TABLE 7

Binding Energies of Co $2p_{3/2}$ Core Level of Co and PtCo Mordenite

Sample	Treatment	Binding energy, eV (FWHM)[a]		Atomic surface ratio	
				Co/Si × 10^3	Si/Al
$Co_{2.91}$-Mor	Fresh (calcined)	782.4 (3.3)	780.2 (2.8)	(36)[b]	(5.8)[b]
		84%[c]	16%[c]	46	6.5
	Fresh (reduced)	782.3 (3.3)	780.2 (2.2)	50	6.1
		86%	14%		
	Used dry	782.1 (3.3)	779.9 (1.9)	30	6.1
		84%	16%		
	Used 2% H_2O	782.2 (3.3)	780.2 (3.1)	30	6.4
		79%	21%		
$Pt_{0.73}Co_{2.6}$-mor (11.7)	Fresh (calcined)	782.2 (3.9)	780.6 (2.8)	(32)[b]	(5.8)[b]
		79%	21%	26	7.0
	Fresh (reduced)	782.5 (3.9)	780.7 (2.6)	24	5.9
		85%	15%		
	Used dry	782.3 (3.3)	780.3 (2.0)	50	5.2
		90%	10%		
$Pt_{4.7}Co_{0.8}$-mor (0.56)	Fresh (calcined)	783.0 (3.3)	780.7 (2.9)	(10)[b]	(5.8)[b]
		62%	38%	22	5.3
	Fresh (reduced) 623 K	783.2 (3.3)	781.3 (2.8)	31	6.0
		46%	54%		
	Fresh (reduced) 843 K	783.0 (3.8)	780.8 (2.5)	26	5.7
		61%	26%		
			778.0 (2.4)		
			13%		

[a] Full width at half-maximum.
[b] Bulk ratio.
[c] Fraction of each component calculated using the XPS peak program.

its Pt $4d_{5/2}$ signal was undetectable. For the $Pt_{0.73}$-mor, the Pt $4f_{7/2}$ peak shows two components at 73.3 and 71.5 eV, and similarly the Pt $4d_{5/2}$ peak shows two components. The Pt species with lower BE had a 53% concentration on the surface which became 100% upon reduction. Vedrine *et al.* (17) reported a BE of 76.4 eV for Pt $4f_{5/2}$, whose Pt $4f_{7/2}$ peak would correspond to a BE of 73.1 eV (assuming a spin–orbit splitting of 3.3 eV for the Pt $4f_{5/2}$–Pt $4f_{7/2}$ levels). They assigned this peak to Pt^{2+} at exchange sites of NaY-zeolite, whereas the peak at 72.2 eV was assigned to metallic Pt particles of 1 to 2 nm. This value is similar to that reported by Zsoldos and Guczi (16).

Vedrine *et al.* (17) reported values of 316.8 eV for Pt^{2+} ions at exchange positions and around 315.0 eV for Pt°. More recent XPS work by Zsoldos *et al.* (18), where the effect of treatment on the Pt^{2+} and Co^{2+} ions exchanged in NaY-zeolite is studied, reports BE values of 316.2 eV for calcined Pt–NaY catalysts and of 314.0 eV for the reduced samples. Similar behavior was observed in the $Pt_{4.7}$-mor sample (not shown).

The Pt $4f_{7/2}$ level of the calcined sample shows two components at BEs of 73.1 and 71.8 eV, whereas after reduction only one at 71.6 eV was observed. If this latter peak were due to metallic Pt, it would be formed during calcination, through the self-reduction of the $Pt(NH_3)_4^{2+}$ ion, to form Pt°. This mechanism has been studied with different Pt-zeolites and it has been shown that under calcination conditions similar to ours (in oxygen flow and low heating rate) the self-reduction process is inhibited (13). However, the appearance of Pt^{2+} species, such as PtO or $Pt(OH)_2$, would occur only by oxidation of the metallic Pt particles.

PtCo-mordenite. The Co $2p_{3/2}$ core-level spectra of $Pt_{0.31}Co_{1.4}$-mor(15) are shown in Fig. 9. All the samples (calcined, reduced, and used) show two components of different intensity and a satellite line. In the calcined sample, both Co $2p_{3/2}$ peaks shift to higher energy values, ca. 783.0 and 780.8 eV. This shift with respect to the values observed in the monometallic $Co_{2.91}$-mor (Table 7) could indicate an interaction between the neighboring Co^{2+} and Pt^{2+} ions located in the zeolitic structure. In the reduced bimetallic Co/Pt = 15 sample, an additional signal is detected at 779.2 eV, which would correspond to metallic cobalt. This is in agreement with the TPR data, which show that part of the cobalt is reduced at temperatures lower than 673 K. The incorporation of platinum increases the reduction of cobalt in the low-temperature zone.

In order to tell whether the reduction performed in the pretreatment chamber of the spectrometer under static conditions is equivalent to the reduction under H_2 flow,

TABLE 8

Binding Energies (BE) of Pt Core Level and Surface Concentrations of Pt and PtCo Mordenites

Sample	Treatment	Binding energy, eV (FWHM)[a]			Surface atomic ratio × 10^3	
		Pt $4f_{7/2}$	Pt $4d_{5/2}$		Pt $4f$/Si	Pt $4d$/Si
$Pt_{0.37}$-mor	Fresh (calcined)	72.4 (2.9)	Undetectable		(1.4)[b]	
					1.7	
	Fresh (reduced)	71.9 (3.3)	Undetectable		(2.0)	0.6
$Pt_{0.73}$-mor	Fresh (calcined)	73.3 (2.3)	317.1 (4.0)	314.2 (2.6)	(2.7)[b]	
		40%[c]	47%	53%		
		71.5 (2.3)			3.0	
		60%				
	Fresh (reduced)	71.3 (2.3)		314.2 (3.1)	4.5	5.0
$Pt_{0.31}Co_{1.4}$-mor(15)	Fresh (calcined)	—	316.0 (1.6)	314.0 (2.0)	(1.3)[b]	0.6
			50%	50%		
	Fresh (reduced)	—	315.6 (2.0)	313.9 (2.2)		3.0
			40%	60%		
	Used dry	71.2 (2.5)	315.9 (2.7)	314.5 (2.6)	6.0	3.3
			37%	63%		
	Used 2% H_2O	71.2 (2.5)	315.7 (2.0)	313.8 (2.4)	4.5	3.5
			15%	85%		
$Pt_{0.73}Co_{2.6}$-mor(11.7)	Fresh (calcined)	71.9 (2.8)	316.8 (2.4)	314.0 (2.2)	(2.9)[b]	
			56%	54%	1.1	1.0
	Fresh (reduced)	72.0 (2.3)	316.8 (3.5)	314.7 (2.6)	1.2	1.2
		71.7 (2.6)	28%	72%		
	Used dry	71.7 (2.8)	316.3 (2.0)	314.9 (2.0)	5.0	4.4
			30%	70%		

[a] Full width at half-maximum.
[b] Bulk ratio.
[c] Fraction of each peak calculated using XPS peak program.

a sample reduced in the flow system was analyzed. The results indicate that the Co state on the surface is virtually the same after both treatments.

When the samples were studied after reaction, the Co $2p_{3/2}$ peak belonging to the metallic Co disappeared and the fraction attributed to Co oxides increased from 25% in the fresh calcined samples to 55 and 35% in the used samples with and without water, respectively. The BE values for the Co–O species of the fresh samples, calcined and reduced (780.8 and 781.0 eV, respectively), were close to that reported for $Co(OH)_2$, 781.0 eV (16). After reaction, the BE of exchanged Co^{2+} was close to the values of the monometallic species.

The Co/Si surface ratio was 0.017 in the bulk and increased up to 0.070 for the used catalysts. This would indicate the migration of Co–O species toward the outer surface during reaction. Table 7 portrays the BE values of Co $2p_{3/2}$ of the bimetallic samples with higher Pt content. It essentially presents the contribution of the two species observed in $Pt_{0.31}Co_{1.4}$-mor(15) (Fig. 9). In $Pt_{0.73}Co_{2.6}$-mor(11.7), the most intense Co $2p_{3/2}$ component according to the different treatments is between 782.2 and 782.5 eV, whereas the least intense signal appears between 780.7 and 780.3 eV. No metallic Co was observed when the sample was reduced at 623 K; Co° was detected only upon reduction at 843 K. The Co/Si ratio increased in the used catalysts. For a high Pt content, $Pt_{4.7}Co_{0.8}$-mor(0.56), the contribution of the Co–O species in the calcined solid was high (38%) and it increased to 54% after reduction.

The BEs of Pt $4f_{7/2}$ and Pt $4d_{5/2}$ levels of the bimetallic samples are shown in Table 8. The $Pt_{0.31}Co_{1.4}$-mor(15) sample, calcined and outgassed in the spectrometer chamber at 623 K, showed two contributions at the Pt $4d_{5/2}$ signal, one around 316.0 eV and the other at 314.0 eV. The lower BE component increased after reaction (2% H_2O). In the $Pt_{0.73}Co_{2.6}$-mor(11.7) sample, the two components of the Pt $4d_{5/2}$ peak at 316.8 and 314.0 eV were similar to those the monometallic sample of comparable concentration ($Pt_{0.73}$-mor). When the bimetallic sample was reduced, the intensity of the peak at 314.0 eV increased. On the other hand, the reduced $Pt_{0.73}$-mor showed only a single peak around 314.2 eV for the Pt $4d_{5/2}$ level and at 71.3 eV for the Pt $4f_{7/2}$ level. The presence of both species, even after reduction, suggests the interaction between Pt and Co, which hinders the complete reduction of Pt^{2+} ions. For the bimetallic sample with a higher Pt content, similar BEs were observed.

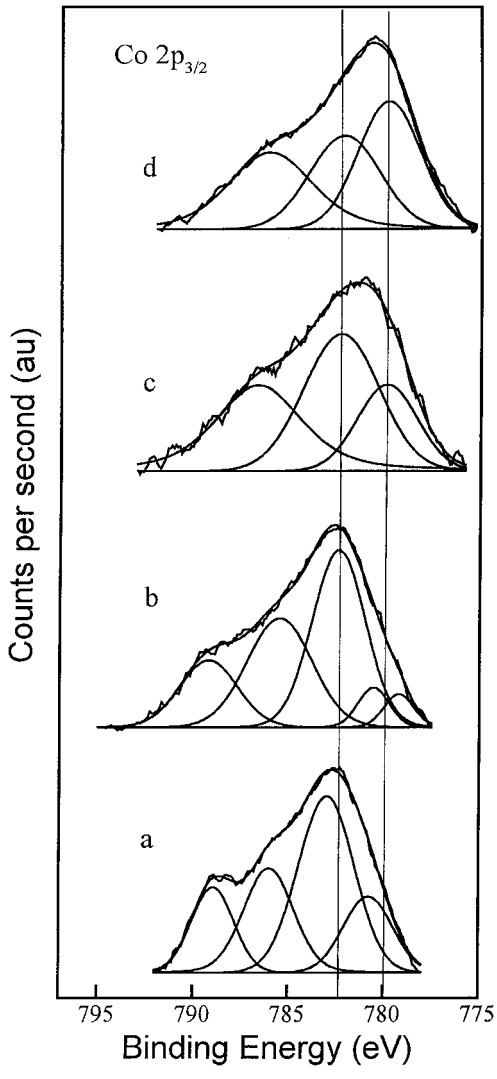

FIG. 9. $Co2p_{3/2}$ core-level spectra of $Pt_{0.31}Co_{1.40}$-mor(15): (a) fresh calcined, (b) fresh reduced in H_2 at 623 K, (c, d) catalyst used in dry and 2% H_2O SCR reaction, respectively.

Pt^{2+} ions at exchange positions were present in both species (316–317 eV), together with metallic Pt. In the $Pt_{4.7}Co_{0.8}$-mor(0.56) sample there appeared an additional component in the Pt $4d_{5/2}$ level around 313.0–313.4 eV, probably corresponding to bigger metallic Pt particles located outside the zeolitic structure. In bimetallic samples with low Pt content, $Pt_{0.73}Co_{2.6}$-mor(11-7) and $Pt_{0.31}Co_{1.40}$-mor(15), calcination and reduction did not change the Pt/Si and Co/Si concentrations with respect to the original one, but after reaction the surface became enriched.

Pt^*Co-mor and Co^*Pt-mor. The XPS results of the samples prepared with an intermediate treatment between exchanges are shown in Table 9. In calcined Pt^*Co-mor the BE values were similar to those recorded in $Pt_{0.31}Co_{1.40}$-mor(15) (Fig. 9). Upon reduction, the Co–O species was apparently the one that was reduced, since the BE changed from 780.1 to 778.2 eV. After use, the cobalt signal became too small, and the peaks could not be identified, whereas two Pt 4*d* signals are detected at 316.6 and 314 eV.

In Co^*Pt-mor the Co–O species did not change with different treatments. However, the component responsible for the Co^{2+} lattice had a value of 782.2 eV in the used sample, similar to that of Co-mor. After exposure to the reacting mixture, the platinum species migrated to the surface while cobalt stayed in the internal channels. In both the used Co^* and Pt^* samples, the Pt migrated toward the external surface. However, the intermediate calcination favored the migration of the Co^{2+} ions to the internal channels of the zeolite, since the Co/Si ratio was lower than that of the bulk (Table 9). This is consistent with the increased resistance to reduction of the used catalysts found in the TPR experiments (Table 6).

DISCUSSION

Our data show that the best catalysts for the SCR of NO_x with CH_4 are those having Co/Pt atomic ratios between 15 and 24 (Fig. 1). These solids, which have been prepared through successive (Pt and Co) ion exchange, achieve high selectivity to N_2 production after being pre-reduced in H_2 at 623 K. All the evidence collected here, and reported in our previous contributions (5–7), indicates, that platinum and cobalt must be in close contact to increase N_2 formation. The following facts support this statement:

- The good catalysts mainly contain Co^{2+}–L and a low proportion of cobalt oxides. This applies to Co-mor and Pt,Co-mor (15/8.5). As a matter of fact, the TPR data indicate that these used solids contain 85%–95% Co^{2+}–L and 5–15% cobalt oxides (Table 4 and Fig. 6).
- Metallic platinum is present at the surface of all the samples shown in Table 8, even before reduction. This Pt° usually forms small clusters. Only at very high Pt concentration ($Pt_{4.7}Co_{0.8}$-mor(0.56)) does the Pt $4d_{5/2}$ spectrum show the appearance of a new component at ca. 313.2 eV, symptomatic of the presence of large Pt° clusters. This catalyst shows low selectivity to N_2 (Fig. 1).
- The bimetallic catalysts were reduced at 623 K to improve performance. However, when the best one, Pt,Co-mor(15), was reduced at 973 K the proportion of Co^{2+}–L drops to 30% (Table 5 and Fig. 7) and the selectivity for N_2 production becomes negligible. Since the $H_2/(Co + Pt)$ ratio is 0.97, it is unlikely that cobalt may have reacted with the lattice to form some sort of cobalt aluminate. This is mentioned here because Yan *et al.* (19) have reported that copper aluminate was detected after NO_x SCR carried on Cu-ZSM5 at 673 K.
- In this same vein, when the catalyst is reduced at 623 K after Pt exchange before exchanging with cobalt (Pt^*Co-mor), the N_2 selectivity drops. The XPS data reveal in this

TABLE 9

XPS Data of Pt*Co and Co*Pt Mordenite Samples

Sample	Treatment	Binding energy, eV (FWHM)[a]				Surface atomic ratio		
		Co $2p_{3/2}$		Pt $4f_{7/2}$	Pt $4d_{5/2}$	Co/Si × 10^3	Pt4f/Si × 10^3	Pt4d/Si × 10^3
$Pt^*_{0.43}Co_{1.31}$-mor(10)	Fresh (calcined)	783.1 (3.9)	780.1 (4.5) 25%[c]	72.04 (2.2)	Undetectable	(16)[b] 20	(2.9)[b] 1.1	(2.9)[b] 1.0
	Fresh (reduced)	783.1 (4.3)	778.2 (3.1) 20%	71.2 (1.6)	315.0 (2.0)	23	1.2	1.2
	Used dry	Noisy[d]		71.6 (2.9)	316.6 (2.5) 314 (2.7) 30%	[d]	5.0	4.4
$Co^*_{2.06}Pt_{0.56}$-mor(10)	Fresh (calcined)	783.0 (3.5)	781.2 (2.4) 12%	72.9 (2.2)	Undetectable	(25)[b] 15	(17)[b] 22	(17)[b] 29
	Fresh (reduced)	783.1 (3.7)	779.7 (3.1) 14%	71.9 (2.5)	Undetectable	19	21	28
	Used dry	782.2 (4.1)	780.0 (2.5) 16%	70.8 (3.1)	316.6 (2.3) 313.8 (2.1) 40%	14	30	35

[a] Full width at half-maximum.
[b] Bulk ratio.
[c] Fraction of each peak calculated using XPS peak program.
[d] The small Co peak area could not be measured.

case that the surface concentration of cobalt is so low that it cannot be detected while the Pt° is now concentrated on the surface of the zeolite crystals (Table 9).

- A similar phenomenon although attenuated occurs when Co is first exchanged and after calcination Pt^{2+} comes in (Co^*Pt-mor). In this case the Pt/Co surface ratio increases (Table 9) and the N_2 selectivity goes down.
- In previous work (7) we have compared the catalytic behavior of mechanical mixtures and two-bed combinations with PtCo-mor ($\geq$15)). The N_2 selectivity was always lower when Pt-mor and Co-mor were used than in those solids where Pt and Co were coexchanged.

In brief, the best catalysts are the product of a right combination of two functions: the selective Co^{2+} occupying exchange positions in the mordenite lattice and highly dispersed Pt° clusters which accelerates the NO oxidation. A high Pt/Co ratio increases the direct reaction of methane with O_2, lowering the N_2 selectivity. Additionally, if the Pt clusters move away from Co^{2+}–L sites and are expelled from the zeolite channels, the selectivity to N_2 is also negatively affected. This view of the bimetallic system is consistent with higher resistance to water poisoning (*vide infra*).

Effect of water. The used catalysts after operation under either dry or wet reaction conditions do not show significantly different TPR profiles and XPS spectra. Particularly, the TPR profiles of PtCo-mor with $11.7 \leq Co/Pt \leq 15$ after either dry or wet reaction are very similar (Fig. 6). For Co/Pt = 8.5, some differences are observed (Fig. 6). The XPS spectra of the $Pt_{0.31}Co_{1.4}$-mor(15) (Fig. 9) show an increase in the proportion of cobalt oxides coming out of the lattice after wet reaction. A similar effect is observed with Pt (Table 8). In the case of Co-mor the same observations are valid.

In view of these results it is concluded that the poisoning effect of water is due to its competitive adsorption on sites that play a role in the SCR of NO_x. This is in agreement with previous findings reported by Li, Battavio, and Armor (1) after studying CoH-ZSM5. The adsorption of water on the Co sites may affect the ability to oxidize NO to NO_2 in the same way as was reported for In-HZSM-5 (20). The noble metal more resistant to water poisoning would provide the active sites for NO oxidation under wet conditions. This would explain why the PtCo-mor is less affected by water vapor than Co-mor (Fig. 2 and Table 2). The overall reversibility of the water poisoning effect when the water addition is stopped (Fig. 3) is also consistent with this general picture.

CONCLUSIONS

The promoting effect of exchanged Pt introduced in cobalt mordenites is now better understood:

—To obtain the best results a close interaction between Co and Pt is needed. Calcination and/or reduction between exchanges or reduction at 973 K leads to preferential platinum expulsion from the zeolite lattice and the consequent drop in selectivity.

—A limited range of Co/Pt ratios (15–24) yields the best selectivity. The presence of Pt in excess reduces the

selectivity because increasing proportions of methane are burned before reacting with NO_x.

—The most selective catalysts contain Co^{2+} at exchange positions plus small clusters of cobalt and platinum oxides. An open question is how these clusters are organized.

—Water competes with NO_x for the adsorption sites, probably decreasing the ability of Co to oxidize NO to NO_2. Pt which is less affected by water still retains the ability to oxidize nitric oxide. The competitive effect of water is supported by the reversibility of the kinetic effect and the absence of any change in solid features after dry and wet reaction.

ACKNOWLEDGMENTS

The authors acknowledge the financial support received from ANPCyT, CONICET, and UNL. Thanks are also given to Prof. Elsa Grimaldi for editing the English manuscript and to Claudio Maitre for his technical support.

REFERENCES

1. Li, Y., Battavio, P., and Armor, J. N., *J. Catal.* **142**, 561 (1993).
2. Armor, J. N., *Catal. Today* **26**, 147 (1995).
3. Porvulerey, V. I., Grange, P., and Dalmon, B., *Catal. Today* **46**, 233 (1998).
4. Amiridis, M. D., Zhang, T., and Farrauto, R. S., *Appl. Catal. B* **10**, 209 (1996).
5. Gutierrez, L., Boix, A., and Petunchi, J., *J. Catal.* **179**, 179 (1998).
6. Gutierrez, L., Boix, A., and Petunchi, J., *Catal. Today* **54**, 451 (1999).
7. Gutierrez, L., Lombardo, E., and Petunchi, J. O., *Appl. Catal. A* **194–195**, 169 (2000).
8. Li, Y., and Armor, J. N., *Appl. Catal. B* **3**, L1 (1993).
9. Zhang, Z., Xu, L., and Sachtler, W., *J. Catal.* **131**, 502 (1991).
10. Boix, A., Ulla, M. A., and Petunchi, J., *J. Catal.* **162**, 239 (1996).
11. Feeley, J., and Sachtler, W., *J. Catal.* **131**, 573 (1991).
12. Feeley, J., and Sachtler, W., *Zeolites* **10**, 738 (1990).
13. Sachtler, W. M. H., and Zhang, Z., *Adv. Catal.* **39**, 129 (1993).
14. Stencel, J. M., Rao, V. U. S., Diehl, J. R., Rhee, K. H., Dhere, A. G., and de Angelis, R. J., *J. Catal.* **84**, 109 (1983).
15. Anderson, S. L. T., and Howe, R. F., *J. Phys. Chem.* **93**, 4913 (1989).
16. Zsoldos, Z., and Guczi, L., *J. Phys. Chem.* **96**, 23 (1992).
17. Vedrine, J. C., Dufaux, M., Naccache, C., and Imelik, B., *J. Chem. Soc., Faraday Trans.* **74**, 440 (1978).
18. Zsoldos, Z., Vass, G., Lu, G., and Guczi, L., *Appl. Surf. Sci.* **78**, 467 (1994).
19. Yan, J. Y., Lei, G. D., Sachtler, W. M. H., and Kung, H. H., *J. Catal.* **161**, 143 (1996).
20. Kikuchi, E., Ogura, M., Aratani, N., Sugiura, Y., Hiromoto, S., and Yogo, K., *Catal. Today* **27**, 35 (1996).